Published for SISSA by Springer

Received: *April 9, 2025*
Revised: *August 10, 2025*
Accepted: *September 13, 2025*
Published: *October 16, 2025*

# Observation of the doubly-charmed-baryon decay $\Xi_{cc}^{++} \to \Xi_c^0 \pi^+ \pi^+$

## The LHCb collaboration

*E-mail:* xingyu.tong@cern.ch

Abstract: A search for the doubly-charmed-baryon decay $\Xi_{cc}^{++} \to \Xi_c^0 \pi^+ \pi^+$ is performed using proton-proton collision data collected by the LHCb experiment at a centre-of-mass energy of 13 TeV and corresponding to an integrated luminosity of $5.4\,\mathrm{fb}^{-1}$. A significant structure consistent with the $\Xi_{cc}^{++}$ baryon is observed in the $\Xi_c^0 \pi^+ \pi^+$ invariant-mass spectrum. Using the $\Xi_{cc}^{++} \to \Lambda_c^+ K^- \pi^+ \pi^+$ decay as the normalisation channel, the branching fraction ratio, $\frac{\mathcal{B}(\Xi_{cc}^{++} \to \Xi_c^0 \pi^+ \pi^+)}{\mathcal{B}(\Xi_{cc}^{++} \to \Lambda_c^+ K^- \pi^+ \pi^+)}$, is measured to be $1.37 \pm 0.18\,(\mathrm{stat}) \pm 0.09\,(\mathrm{syst}) \pm 0.35\,(\mathrm{ext})$. This measurement provides critical input for testing QCD factorisation methods in the weak decays of doubly-heavy baryons, particularly in quantifying nonperturbative effects such as final-state interactions and resonance contributions to the hadronisation process.

Keywords: Branching fraction, Charm Physics, Hadron-Hadron Scattering, QCD

ArXiv ePrint: 2504.05063

Open Access, Copyright CERN,
for the benefit of the LHCb Collaboration.
Article funded by SCOAP$^3$.

https://doi.org/10.1007/JHEP10(2025)136

JHEP10(2025)136

## Contents


**1 Introduction** 1

**2 Detector, trigger and simulation** 3

**3 Event selection** 4

**4 Mass distributions and signal significance** 5

**5 Efficiencies** 7

**6 Systematic uncertainties** 8

**7 Result and conclusion** 10

**The LHCb collaboration** 15


## 1 Introduction

In the quark model [1–3], hadrons are arranged into multiplets according to the symmetry properties of their wave functions in terms of the flavour, spin and colour quantum numbers of the constituent quarks. When four quark flavours, namely $u$, $d$, $s$ and $c$, are considered, hadrons form SU(4) multiplets [4]. Within these multiplets, all predicted ground-state baryons with charm quantum numbers $C = 0$ and $C = 1$ have been observed [5], and three weakly decaying baryons with $C = 2$ are expected, $\Xi_{cc}^{++}(ccu)$, $\Xi_{cc}^{+}(ccd)$ and $\Omega_{cc}^{+}(ccs)$, collectively referred to as doubly charmed baryons.[1] These states provide unique information on the dynamics of low-energy interactions between two heavy quarks in a confined object, yielding new important insights on the theory of quantum chromodynamics (QCD).

In 2017, the LHCb collaboration reported the observation of a significant structure in the $\Lambda_c^+ K^- \pi^+ \pi^+$ mass spectrum, consistent with originating from the doubly charmed baryon $\Xi_{cc}^{++}$ [6]. The $\Xi_{cc}^{++}$ baryon was later confirmed in $\Xi_{cc}^{++} \to \Xi_c^+ \pi^+$ [7] and $\Xi_{cc}^{++} \to \Xi_c'^+ \pi^+$ decays [8], while no significant signal was found in a search for $\Xi_{cc}^{++} \to D^+ p K^- \pi^+$ decays [9]. The production cross-section of the $\Xi_{cc}^{++}$ baryon times the branching fraction of the $\Xi_{cc}^{++} \to \Lambda_c^+ K^- \pi^+ \pi^+$ decay has been measured with respect to that of the $\Lambda_c^+$ baryon, in proton-proton ($pp$) collisions at a centre-of-mass energy of 13 TeV [10]. Its lifetime and mass have been determined to be $0.256^{+0.024}_{-0.022}\,(\text{stat}) \pm 0.014\,(\text{syst})$ ps [11] and $3621.55 \pm 0.23\,(\text{stat}) \pm 0.30\,(\text{syst})\,\text{MeV}/c^2$ [12], respectively, which are consistent with a range of theoretical predictions obtained with various methods including heavy quark effective theory (HQET) [13], QCD sum rules [14, 15], perturbative QCD [16], lattice QCD [17], and relativistic quark model [18]. Nevertheless, only three decay modes of the $\Xi_{cc}^{++}$ baryon have been observed so far, although many more have been predicted [19–22]. Measurements of additional $\Xi_{cc}^{++}$

[1] Charge conjugated states are included throughout this paper unless otherwise stated.



JHEP10(2025)136

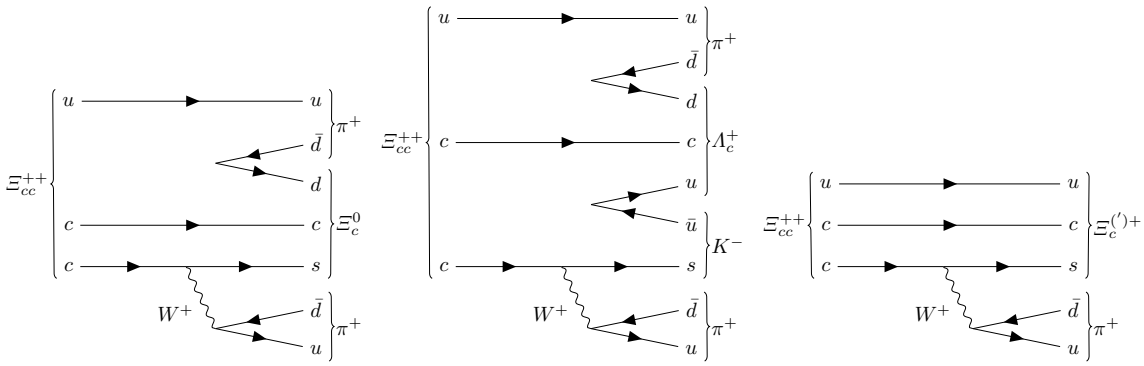


**Figure 1.** Examples of diagrams contributing to (left) $\Xi_{cc}^{++} \to \Xi_c^0\pi^+\pi^+$, (middle) $\Xi_{cc}^{++} \to \Lambda_c^+K^-\pi^+\pi^+$ and (right) $\Xi_{cc}^{++} \to \Xi_c^{(\prime)+}\pi^+$ decays.

decay modes provide essential information to better understand the decay dynamics of doubly charmed baryons [23].

This paper reports the first observation of the $\Xi_{cc}^{++} \to \Xi_c^0\pi^+\pi^+$ decay in $pp$ collision data collected by the LHCb experiment at a centre-of-mass energy of 13 TeV, corresponding to an integrated luminosity of $5.4\,\text{fb}^{-1}$. The $\Xi_{cc}^{++} \to \Xi_c^0\pi^+\pi^+$ decay is mediated by the same $c \to s u \bar{d}$ weak transition as for the known $\Xi_{cc}^{++} \to \Lambda_c^+K^-\pi^+\pi^+$ and $\Xi_{cc}^{++} \to \Xi_c^{(\prime)+}\pi^+$ decays, as shown in figure 1. However, the formation of additional quark-antiquark pairs and the subsequent hadronisation dynamics are dominated by nonperturbative strong interactions [24, 25]. Theoretical prediction of the branching fraction is challenged by the interplay of multiple factors: (i) Coupled-channel interference mediated by resonances in the multi-body phase space [26], (ii) limited predictive power of QCD factorisation near the charm-quark mass scale ($m_c \sim 1.5\,\text{GeV}/c^2$), and (iii) the violation of heavy quark symmetry of HQET in the doubly heavy baryon system [27]. Therefore, measurement of the branching fractions can help to understand the nonperturbative interactions in the weak decays of doubly heavy baryons.

The branching fraction of the $\Xi_{cc}^{++} \to \Xi_c^0\pi^+\pi^+$ decay is measured relative to the normalisation channel $\Xi_{cc}^{++} \to \Lambda_c^+K^-\pi^+\pi^+$. The $\Xi_c^0$ and $\Lambda_c^+$ baryons in the signal and normalisation channels are reconstructed via the $pK^-K^-\pi^+$ and $pK^-\pi^+$ final states, respectively. The branching fraction ratio is defined and measured according to

$$\mathcal{R} \equiv \frac{\mathcal{B}(\Xi_{cc}^{++} \to \Xi_c^0\pi^+\pi^+) \times \mathcal{B}(\Xi_c^0 \to pK^-K^-\pi^+)}{\mathcal{B}(\Xi_{cc}^{++} \to \Lambda_c^+K^-\pi^+\pi^+) \times \mathcal{B}(\Lambda_c^+ \to pK^-\pi^+)} = \frac{N_{\text{sig}}}{N_{\text{norm}}} \times \frac{\varepsilon_{\text{norm}}}{\varepsilon_{\text{sig}}},$$

where $\mathcal{B}$ denotes the branching fraction of the relevant decay mode, and $N_{\text{sig(norm)}}$ and $\varepsilon_{\text{sig(norm)}}$ are the yield and efficiency for the signal (normalisation) channel, respectively. Compared to $\Lambda_c^+$, the $\Xi_c^0$ baryon has a shorter lifetime, resulting in significantly lower detection efficiency. The smaller branching fraction of $\Xi_c^0 \to pK^-K^-\pi^+$ makes the study of the $\Xi_{cc}^{++} \to \Xi_c^0\pi^+\pi^+$ decay more challenging. However, since the final-state particles in the two $\Xi_{cc}^{++}$ decays are exactly the same, many systematic uncertainties cancel in the ratio of branching fractions. In order to avoid experimenter's bias, the results of the analysis were not examined until the full procedure had been finalised.



JHEP10(2025)136

## 2 Detector, trigger and simulation

The LHCb detector [28, 29] is a single-arm forward spectrometer covering the pseudorapidity range $2 < \eta < 5$, designed for the study of particles containing $b$ or $c$ quarks. The detector includes a high-precision tracking system consisting of a silicon-strip vertex detector surrounding the $pp$ interaction region [30], a large-area silicon-strip detector located upstream of a dipole magnet with a bending power of about 4 T m, and three stations of silicon-strip detectors and straw drift tubes [31] placed downstream of the magnet. The tracking system provides a measurement of the momentum, $p$, of charged particles with a relative uncertainty that varies from 0.5% at 2 GeV/$c$ to 1.0% at 200 GeV/$c$. The minimum distance of a track to a primary $pp$ collision vertex (PV), the impact parameter (IP), is measured with a resolution of $(15 + 29/p_{\mathrm{T}})$ µm, where $p_{\mathrm{T}}$ is the component of the momentum transverse to the beam, in GeV/$c$. Different types of charged hadrons are distinguished using information from two ring-imaging Cherenkov (RICH) detectors [32]. Photons, electrons and hadrons are identified by a calorimeter system consisting of scintillating-pad and preshower detectors, an electromagnetic and a hadronic calorimeter. Muons are identified by a system composed of alternating layers of iron and multiwire proportional chambers [33].

The online event reconstruction and selection are performed by a trigger [34], which consists of a hardware and a software level. At the hardware level, events are triggered if they contain a muon with high $p_{\mathrm{T}}$, or a hadron, photon, or electron with high transverse energy in the calorimeters. A $\Xi_{cc}^{++}$ candidate is required to have a positive hardware trigger decision, either due to particles from the signal decay (Trigger-On-Signal, TOS), or due to particles in the rest of the event (Trigger-Independent-of-Signal, TIS). Due to the different size of systematic uncertainties induced by the hardware trigger requirement, candidates are divided into two disjoint categories, denoted as TIS and exTOS, where the latter includes candidates that are selected by the TOS but not by the TIS requirement. The branching fraction ratio is measured independently for each trigger category, and the baseline result comes from the combination of the two measurements.

The software trigger is divided into two stages. The first stage selects a single particle with large $p_{\mathrm{T}}$ and significant separation from all PVs in the event, or a two-particle vertex displaced from the PV. In the second software trigger stage, the full event reconstruction and selection is performed [35]. Using $p$, $K^-$ and $\pi^+$ hadrons that are well identified by the RICH detectors, $\Xi_c^0$ candidates are built by forming $pK^-K^-\pi^+$ particle combinations. The proton is required to have $p > 10$ GeV/$c$ to ensure valid particle identification (PID) information [32]. All particles in the $\Xi_c^0$ final state must have a good track-fit quality, $p_{\mathrm{T}} > 500$ MeV/$c$, and $\chi^2_{\mathrm{IP}} > 6$ with respect to any PVs, where $\chi^2_{\mathrm{IP}}$ is defined as the difference in the vertex-fit $\chi^2$ of a given PV reconstructed with and without the particle under consideration. Additionally, at least one of the four final-state particles must have $p_{\mathrm{T}} > 1$ GeV/$c$ and $\chi^2_{\mathrm{IP}} > 8$. The scalar sum of $p_{\mathrm{T}}$ of the four final-state particles must be greater than 3 GeV/$c$. The $\Xi_c^0$ candidate must have a good vertex-fit quality, and the vertex must be displaced from the associated PV with a distance corresponding to a decay time of at least 0.1 ps. The associated PV is the one that best fits the flight direction of the reconstructed candidate. Each $\Xi_c^0$ candidate is combined with two $\pi^+$ mesons to form a $\Xi_{cc}^{++}$ candidate. The two pions are required to have $p_{\mathrm{T}} > 200$ MeV/$c$ and good track-fit quality. The $\Xi_{cc}^{++}$ candidates must



JHEP10(2025)136

have a good vertex-fit quality, and the vertex of the $\Xi_c^0$ baryon must be located downstream than that of the $\Xi_{cc}^{++}$ baryon.

The selection criteria for the normalisation channel are similar to those for the signal decay. Appropriate adjustments on the thresholds are made taking into account the differences due to the intermediate $\Lambda_c^+$ and $\Xi_c^0$ baryons.

The momentum scale is calibrated using samples of $J/\psi \to \mu^+\mu^-$ and $B^+ \to J/\psi K^+$ decays collected concurrently with the data sample used for this analysis [36, 37]. The relative accuracy of the calibration is estimated to be $3 \times 10^{-4}$ using samples of other fully reconstructed decays of beauty hadrons and $K_S^0$ mesons.

Simulated $\Xi_{cc}^{++}$ decays are used to optimise the event selections, study the signal invariant-mass distributions, and evaluate the efficiencies used for the measurement of the relative branching fraction. In the simulation, $pp$ collisions are generated using Pythia [38, 39] with a specific LHCb configuration [40]. A dedicated generator for doubly heavy baryon production, GenXicc 2.0 [41], is used to produce the $\Xi_{cc}^{++}$ baryons. Decays of unstable particles are described by EvtGen [42], in which final-state radiation is generated using Photos [43]. The interaction of the generated particles with the detector, and its response, are implemented using the Geant4 toolkit [44, 45] as described in ref. [46]. In the simulation, $\Xi_{cc}^{++}$ baryons are generated with a mass of $3621\,\mathrm{MeV}/c^2$ and a lifetime of $0.256\,\mathrm{ps}$ [11, 12]. The decay products of the $\Xi_{cc}^{++}$ baryons are uniformly distributed in the allowed phase space. The singly charmed $\Xi_c^0$ decays are distributed according to a pseudoresonant model in which half of the $\Xi_c^0$ decays proceed through the resonant decay $\Xi_c^0 \to pK^-\overline{K}^*(892)^0$ followed by the decay of the $\overline{K}^*(892)^0$ meson to the $K^-\pi^+$ final state [5], while the others are uniformly distributed in the phase space. For the normalisation channel, the decay products of the $\Xi_{cc}^{++}$ baryons are uniformly distributed in the allowed phase space, while the $\Lambda_c^+$ baryons are assumed to decay via a four-component pseudoresonant model, which includes the phase-space decay, and the $p\overline{K}^*(892)^0$, $\Lambda(1520)\pi^+$, and $\Delta(1232)^{++}K^-$ resonant processes.

## 3 Event selection

The event selection is performed in three steps: a preselection, a multivariate analysis, and the veto of physics background. In the preselection, each particle in the $\Xi_{cc}^{++}$ final state is required to have a momentum within $[2, 150]\,\mathrm{GeV}/c$ and pseudorapidity within $[1.6, 5.3]$. The $\Xi_{cc}^{++}$ candidate is required to originate from its associated PV. The invariant mass of $pK^-K^-\pi^+$ from the $\Xi_c^0$ candidate is required to be within $[2453, 2489]\,\mathrm{MeV}/c^2$, which corresponds to $\pm 3$ times the mass resolution around the known mass [5]. The $\Xi_{cc}^{++}$ candidates reconstructed in the signal and normalisation samples are required to have rapidity within $[2, 4.5]$ and transverse momentum within $[4, 15]\,\mathrm{GeV}/c$.

The combinatorial background is further suppressed with a boosted decision tree (BDT) [47, 48] classifier implemented in the TMVA toolkit [49, 50]. The classifier is trained using simulated decays as a signal proxy and the $\Xi_c^0\pi^+\pi^-$ wrong-sign (WS) sample with the mass in the region of $[3501, 3741]\,\mathrm{MeV}/c^2$ as a background proxy. The BDT training exploits the differences between signal and background candidates in the distributions of the fit qualities of $\Xi_{cc}^{++}$ and $\Xi_c^0$ decay vertices, the $\chi^2_{\mathrm{IP}}$ and $p_{\mathrm{T}}$ of $\Xi_{cc}^{++}$ and $\Xi_c^0$ candidates and their decay products, the angle between the momentum and the vector formed by the PV and the



JHEP10(2025)136

decay vertex for $\Xi_{cc}^{++}$ and $\Xi_c^0$ candidates. The PID information calibrated from data [51] of all final-state particles is also exploited, which discriminates between pion, kaon and proton particles. The same procedure is performed for the signal and normalisation decays.

The requirement in the output of the BDT classifier for the signal channel is optimised using the Punzi figure of merit $\varepsilon_{\rm sig}/(n_\sigma/2+\sqrt{N_{\rm bkg}})$ [52], where $\varepsilon_{\rm sig}$ is the signal efficiency obtained from simulation, and $n_\sigma = 5$ corresponds to the target significance of five standard deviations. The background yield in the signal region of $\pm 15\,{\rm MeV}/c^2$ around the known $\Xi_{cc}^{++}$ mass [5], denoted as $N_{\rm bkg}$, is estimated by counting the WS yield in the signal region and scaling it by the yield ratio of right-sign and wrong-sign data in the mass region $[3750, 3800]\,{\rm MeV}/c^2$. The optimal BDT selection corresponds to a signal efficiency of approximately 65% and a background rejection of approximately 99%. For the normalisation channel, the working point of the classifier is chosen to have the same BDT efficiency as the signal channel to minimise the systematic uncertainty.

The normalisation decay $\Xi_{cc}^{++} \to \Lambda_c^+(\to pK^-\pi^+)K^-\pi^+\pi^+$ can be misreconstructed as the signal decay if the $\Lambda_c^+$ decay products are combined with particles produced promptly from the $\Xi_{cc}^{++}$ decay to form a $\Xi_c^0$ candidate. This physics background component peaks in the $\Xi_{cc}^{++}$ invariant-mass distribution and is suppressed to a negligible level by vetoing $pK^-\pi^+$ candidates with invariant masses within $[2268, 2304]\,{\rm MeV}/c^2$, i.e. consistent with the known $\Lambda_c^+$ mass [5]. The efficiency of this requirement for the signal decay is about 80%, estimated from simulation.

## 4 Mass distributions and signal significance

In order to improve the mass resolution [12], the invariant mass of the $\Xi_{cc}^{++}$ candidate is measured as

$$m_{\rm cand}\left(\Xi_c^0\pi^+\pi^+\right) \equiv m\left(\Xi_c^0\pi^+\pi^+\right) - m\left(\Xi_c^0\right) + M_{\rm PDG}\left(\Xi_c^0\right),$$

for the signal channel, where $m\left(\Xi_c^0\pi^+\pi^+\right)$ and $m\left(\Xi_c^0\right)$ are the invariant mass of the $\Xi_c^0\pi^+\pi^+$ and $pK^-K^-\pi^+$ systems, respectively, and $M_{\rm PDG}\left(\Xi_c^0\right)$ is the known mass of the $\Xi_c^0$ baryon [5]. For the normalisation channel, an analogous definition of

$$m_{\rm cand}\left(\Lambda_c^+K^-\pi^+\pi^+\right) \equiv m\left(\Lambda_c^+K^-\pi^+\pi^+\right) - m\left(\Lambda_c^+\right) + M_{\rm PDG}\left(\Lambda_c^+\right),$$

is adopted. The distributions of the invariant mass of the $pK^-K^-\pi^+$ and the $\Xi_c^0\pi^+\pi^+$ systems are shown in figure 2. A significant structure can be seen in the $\Xi_c^0\pi^+\pi^+$ invariant-mass distribution at a mass of approximately $3620\,{\rm MeV}/c^2$. No significant structure is visible in the WS sample, nor in the sample with $\Xi_c^0$ candidates in the mass sidebands given by $[2401, 2441] \cup [2501, 2541]\,{\rm MeV}/c^2$.

An unbinned maximum-likelihood fit is performed simultaneously to the invariant-mass distributions of the $\Xi_{cc}^{++}$ candidates for the signal and normalisation channels. In both channels, the $\Xi_{cc}^{++}$ contribution is described with the sum of a Gaussian function and a double-sided Crystal Ball (DSCB) function [53], with the fraction of the DSCB and the Gaussian fixed to the value obtained in simulation, and the combinatorial background is described with a first-order polynomial. The shape parameters of the DSCB function are



JHEP10(2025)136

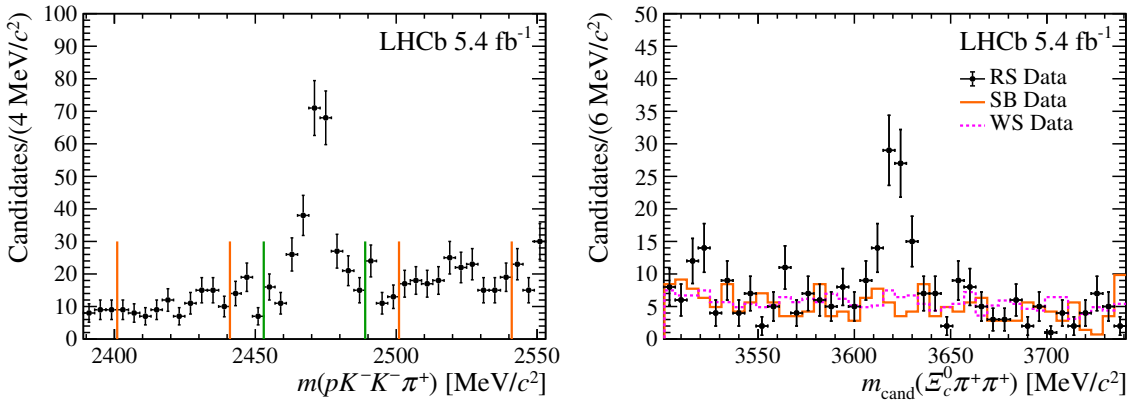


**Figure 2.** Distributions of the invariant mass of the (left) $pK^-K^-\pi^+$ and (right) $\Xi_c^0\pi^+\pi^+$ systems. In the left plot, the boundary of the signal and sideband mass regions of the $\Xi_c^0$ candidates are indicated by green and orange lines, respectively. In the right plot, the right-sign (RS) signal decays are shown in black points, along with the sample with $\Xi_c^0$ candidates in the mass sidebands (SB) in pink dashed line and the sample with wrong-sign (WS) combinations in orange solid line, both normalised to have the same area as the RS sample in the $m_{\rm cand}\left(\Xi_c^0\pi^+\pi^+\right)$ sidebands given by $[3501, 3561] \cup [3681, 3741]$ MeV/$c^2$.

| Category | $N_{\rm sig}$ | $N_{\rm norm}$ | $\varepsilon_{\rm sig}$ $[\times 10^{-4}]$ | $\varepsilon_{\rm norm}$ $[\times 10^{-4}]$ |
|---|---|---|---|---|
| TIS | $62 \pm 9$ | $1279 \pm 55$ | $1.159 \pm 0.023$ | $2.547 \pm 0.090$ |
| exTOS | $21 \pm 6$ | $461 \pm 34$ | $0.286 \pm 0.011$ | $0.624 \pm 0.034$ |

**Table 1.** Yields and efficiencies of the signal and normalisation channels. The uncertainties on the yields are statistical only; the uncertainties on the efficiencies include only the contribution from the limited size of the simulation sample.

fixed to the values obtained from simulation, except for the peak position and width, while the parameters of the polynomial background function are free to vary. For the signal channel, there is a contribution from the partially reconstructed $\Xi_{cc}^{++} \to \Xi_c'^0(\to \Xi_c^0\gamma)\pi^+\pi^+$ decay, whose shape is obtained using simulated samples generated with RapidSim [54] and fixed in the fit. In the simultaneous fit, the signal and normalisation channels share the same peak position, and the ratio of the peak widths is fixed to the value obtained from the simulation. Figure 3 shows the invariant-mass distributions of the $\Xi_{cc}^{++}$ candidates in both signal and normalisation channels, along with the fit results. The significance of the $\Xi_{cc}^{++} \to \Xi_c^0\pi^+\pi^+$ signal is estimated to be above $10\sigma$ according to Wilks' theorem [55], taking into account the systematic uncertainty due to the fit model, while the partially reconstructed $\Xi_{cc}^{++} \to \Xi_c'^0(\to \Xi_c^0\gamma)\pi^+\pi^+$ component is not significant. Simultaneous fits are then performed for the TIS and exTOS trigger categories separately, from which the signal yields are obtained and summarised in table 1.

The background-subtracted invariant-mass distributions of the two $\Xi_c^0\pi^+$ systems in the signal $\Xi_{cc}^{++} \to \Xi_c^0\pi^+\pi^+$ decay are obtained using the *sPlot* [56] method with $m_{\rm cand}\left(\Xi_c^0\pi^+\pi^+\right)$ as the discriminating variable. No significant narrow $\Xi_c^+$ excited states are observed.



JHEP10(2025)136

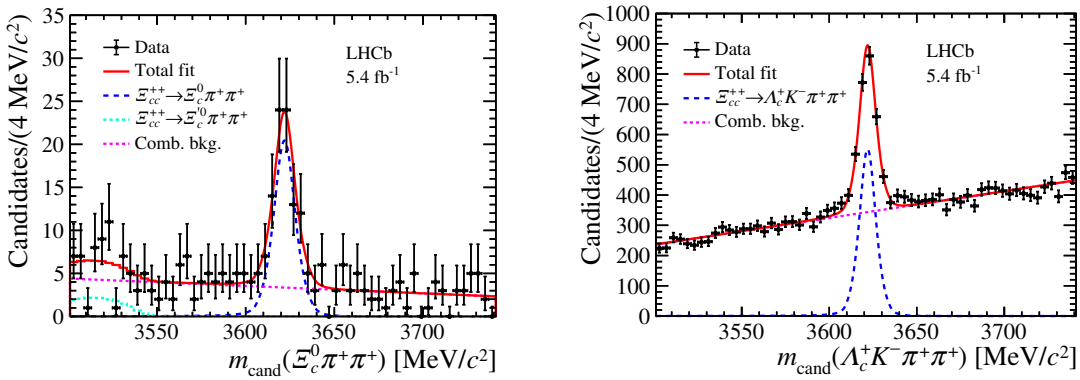


**Figure 3.** Distributions of the invariant masses of the (left) $\Xi_c^0\pi^+\pi^+$ and (right) $\Lambda_c^+K^-\pi^+\pi^+$ systems, along with the result of the simultaneous fit.

## 5 Efficiencies

Simulated samples of the signal and normalisation channels are used to evaluate the reconstruction and selection efficiencies. Corrections are applied to these samples to ensure that the quantities which affect the efficiency determination are well described by the simulation. Namely, the charged particle multiplicity and the $\Xi_{cc}^{++}$ transverse-momentum distributions of the simulation sample are corrected to match those of the normalisation channel data. In addition, track-momentum- and pseudorapidity-dependent corrections are applied to better match the PID response and tracking efficiency in data, as described in refs. [51, 57]. The phase-space distributions of the $\Xi_{cc}^{++}\to\Lambda_c^+K^-\pi^+\pi^+$, $\Lambda_c^+\to pK^-\pi^+$ and $\Xi_c^0\to pK^-K^-\pi^+$ decays in the simulation samples are weighted to match the data [58]. The $\Xi_{cc}^{++}\to\Lambda_c^+K^-\pi^+\pi^+$ and $\Lambda_c^+\to pK^-\pi^+$ phase-space distributions in the data are taken from the normalisation decay, while the $\Xi_c^0\to pK^-K^-\pi^+$ phase-space distributions is taken from that of the $\Xi_c^0$ baryon in the abundant $\Xi_b^-\to\Xi_c^0\pi^-$ decay [59]. After implementing these corrections, the simulation and data for the signal channel show a high degree of agreement. However, a discrepancy remains in the efficiency of the BDT selection for the normalisation channel. To investigate this, a looser BDT selection is applied while maintaining a discernible peak in the $m_{\rm cand}\left(\Lambda_c^+K^-\pi^+\pi^+\right)$ spectrum of the data. This discrepancy is corrected by multiplying the efficiency for the normalisation channel by a factor,

$$f_{\rm BDT}=\frac{\varepsilon_{\rm data}(\text{Nominal BDT}|\text{Looser BDT})}{\varepsilon_{\rm sim}(\text{Nominal BDT}|\text{Looser BDT})},$$

where $\varepsilon_{\rm data(sim)}(\text{Nominal BDT}|\text{Looser BDT})$ is the efficiency of the nominal BDT requirement, given that the looser BDT requirement has been applied, for the data (simulation) samples. The correction factor is determined to be $0.90\pm0.04$, where the uncertainty is systematic as discussed in section 6. The background-subtracted distributions in data are determined with the *sPlot* method.

The total efficiencies after corrections for the signal and normalisation channels and for the two hardware trigger categories are shown in table 1, from which the efficiency ratios between the signal and the normalisation channel are determined to be $0.454\pm0.019$ and



JHEP10(2025)136

| Source | TIS(%) | exTOS(%) |
|---|---|---|
| Fit model | 1.1 | 1.1 |
| Simulation sample size | 4.2 | 6.6 |
| $\Xi_{cc}^{++}$ lifetime | 1.0 | 1.0 |
| Kinematic correction | 1.2 | 1.2 |
| Decay dynamics | 2.0 | 2.0 |
| Tracking | 1.5 | 1.5 |
| Particle identification | 1.4 | 1.4 |
| Hardware trigger | — | 9.0 |
| Hit error parametrisation | 0.5 | 0.5 |
| BDT efficiency correction | 4.4 | 4.4 |
| Total | 7.0 | 12.5 |

**Table 2.** Summary of the relative systematic uncertainties on the branching fraction ratio $\mathcal{R}$.

$0.458 \pm 0.030$ for the TIS and exTOS categories, respectively. The uncertainties are attributed to the limited size of the simulation samples only.

## 6 Systematic uncertainties

The branching fraction ratio measurement has systematic uncertainties arising from determinations of the relative yields and relative efficiencies, as summarised in table 2 and described below. Individual systematic uncertainties are added in quadrature to obtain the total uncertainty, and determined to be 7.0% and 12.5% for the TIS and exTOS samples, respectively.

The models used in the fits to the invariant-mass distributions may bias the relative signal yields. This systematic uncertainty is studied by using alternative functions to describe the shapes of the $\Xi_{cc}^{++}$ and background components simultaneously for the signal and normalisation channels. The sum of two Gaussian functions is chosen as the $\Xi_{cc}^{++}$ model, the second-order polynomial function is chosen as the alternative combinatorial background model, and a third alternative model is the baseline model excluding the partially reconstructed component of the signal channel. The change in the yield ratio is assigned as the systematic uncertainty for each alternative model, and the sum in quadrature of the three sources is 1.1%.

Three categories of systematic uncertainty arising from the determination of the relative efficiencies are evaluated. First, the uncertainty due to the limited size of the simulated samples is evaluated to be 4.2% and 6.6% for the TIS and the exTOS result, respectively.

The second category is due to the imperfect or missing knowledge of the $\Xi_{cc}^{++}$ baryon properties, including its lifetime and kinematic distributions, and the resonant structure of $\Xi_{cc}^{++} \to \Xi_c^0 \pi^+ \pi^+$ and $\Xi_{cc}^{++} \to \Lambda_c^+ K^- \pi^+ \pi^+$ decays. The uncertainty in the selection efficiency due to the imprecise $\Xi_{cc}^{++}$ lifetime [5, 11] is evaluated by weighting the simulation samples to match the known $\Xi_{cc}^{++}$ lifetime values varied within $\pm 1$ standard deviation. The largest relative variation in the efficiency ratio, 1.0%, is assigned as a systematic uncertainty. The systematic uncertainty associated with the $\Xi_{cc}^{++}$ kinematic corrections is tested with simulations. For each test, the simulated samples are weighted to match a specific kinematic distribution, where the correction factor in each transverse-momentum interval of the $\Xi_{cc}^{++}$ baryon and the



JHEP10(2025)136

charged particle multiplicity interval is varied according to a Gaussian distribution defined by the nominal value and its uncertainty. The width of the resulting distribution of the efficiency ratio in different tests is assigned as the corresponding systematic uncertainty, which is 1.2%. The dynamics of the $\Xi_{cc}^{++} \to \Xi_c^0\pi^+\pi^+$ decay is characterised by the resonant structures and the polarisation of each quasi-two-body decay chain. Variation of the efficiency due to possible resonant enhancements is studied by measuring the efficiency in regions of Dalitz-plot variables $(m_l(\Xi_c^0\pi^+), m_h(\Xi_c^0\pi^+))$ and performing event-by-event efficiency corrections using the two-dimensional efficiency map, where the subscript $l$ ($h$) refers to the lower (higher) value of the two $\Xi_c^0\pi^+$ invariant masses. The relative difference between the nominal efficiency and the per-event-corrected efficiency is taken as the uncertainty due to resonant structures. The systematic uncertainty associated with the polarisation is also studied with simulations. The $\Xi_{cc}^{++} \to \Xi_c^0(\to pK^-K^-\pi^+)\pi^+\pi^+$ decay can be expressed as the coherent sum of sequential two-body decays [60]. A series of tests are performed using the fully simulated samples weighted to match various polarisations, in which the helicity amplitudes of each two-body decay chain are randomly assigned. The width of the resulting distribution of the efficiencies is taken as the systematic uncertainty due to the unknown polarisation. The systematic uncertainty due to the decay dynamics is the sum in quadrature of the uncertainties from the resonant structures and the polarisation, and amounts to 2.0%.

The third category of systematic uncertainty accounts for the discrepancy between data and simulation, including effects due to tracking, particle identification, the hardware trigger, the hit error parametrisation of the vertex detector, and the BDT efficiency. The systematic uncertainty associated with the tracking efficiency stems from the limited size of the calibration data samples used to measure it [57], and is evaluated to be 1.5%. The systematic uncertainty associated with the PID correction is evaluated using alternative calibration samples in the PID correction procedure [51]. The maximum relative change of the branching fraction ratio, 1.4%, is assigned as the uncertainty from this procedure. The inconsistency of hit error parametrisation of the vertex detector between simulation and data leads to a small discrepancy in $\chi^2_{\rm IP}$ distributions, and hence biases the efficiency. The impact on the efficiency ratio is assessed by scaling the $\chi^2_{\rm IP}$ values of the final-state particles in simulation using a factor estimated conservatively based on the observed behaviour of the vertex detector. The relative change in the efficiency ratio between the signal and normalisation channels is 0.5%, which is taken as the systematic uncertainty. The uncertainty due to the simulation of the hardware trigger is evaluated for TIS and exTOS data samples, separately. For the exTOS sample, a data-driven method is used to determine the TOS efficiency as a function of the energy deposited in the hadronic calorimeter by each final-state particle [34, 61]. The difference in the ratio of TOS efficiencies between the baseline value and the one obtained with the data-driven method, 9.0%, is taken as the systematic uncertainty for the exTOS sample. The TIS sample is independent of the $\Xi_{cc}^{++}$ decay by construction. Since the kinematic of $\Xi_{cc}^{++}$ and the charged particle multiplicity have been corrected and corresponding systematic uncertainties are studied, no extra systematic uncertainty is assigned to this sample. In the baseline procedure, a looser BDT requirement is used to correct the BDT efficiency of the normalisation channel. However, the efficiency of this looser BDT requirement may differ between the simulation and the data. To investigate the uncertainty associated with this procedure, a traditional selection method without machine learning is used in place of the



JHEP10(2025)136

looser BDT requirement to derive the correction factor. The difference between the baseline value and the one obtained with the alternative selection, 4.4%, is taken as the uncertainty due to the correction of the BDT efficiency.

## 7 Result and conclusion

Taking into account the ratios of the $\Xi_{cc}^{++}$ yields and efficiencies between the signal and normalisation channels, and associated uncertainties, the branching fraction ratio is measured to be

$$\mathcal{R} = 0.107 \pm 0.016(\text{stat}) \pm 0.007(\text{syst}), \text{ for the TIS sample,}$$
$$\mathcal{R} = 0.100 \pm 0.029(\text{stat}) \pm 0.012(\text{syst}), \text{ for the exTOS sample.}$$

The measurements from the two samples are consistent and are combined using the best linear unbiased estimator [62, 63] to obtain

$$\mathcal{R} = 0.105 \pm 0.014(\text{stat}) \pm 0.007(\text{syst}).$$

In the combination, systematic uncertainties arising from the limited size of the simulated samples are assumed to be uncorrelated between the TIS and exTOS categories, while the remaining nonzero systematic uncertainties are taken to be fully correlated.

Using the measured branching fractions of $\Lambda_c^+ \to pK^-\pi^+$ and $\Xi_c^0 \to pK^-K^-\pi^+$ decays [5], the branching fraction ratio of the two doubly charmed baryon decays is measured to be

$$\frac{\mathcal{B}(\Xi_{cc}^{++} \to \Xi_c^0\pi^+\pi^+)}{\mathcal{B}(\Xi_{cc}^{++} \to \Lambda_c^+K^-\pi^+\pi^+)} = 1.37 \pm 0.18(\text{stat}) \pm 0.09(\text{syst}) \pm 0.35(\text{ext}),$$

where the external uncertainty comes from those on the branching fractions of the $\Lambda_c^+ \to pK^-\pi^+$ and $\Xi_c^0 \to pK^-K^-\pi^+$ decays [5]. Taking into account the contributions of two, three and four-body decays [21, 22, 26, 64, 65], the measured relative branching fraction is consistent with theoretical predictions. Moreover, unlike the $\Xi_{cc}^{++} \to \Lambda_c^+K^-\pi^+\pi^+$ decay, the $\Xi_{cc}^{++} \to \Xi_c^0\pi^+\pi^+$ decay is found to be almost a nonresonant process, and thus is a good channel to test the QCD factorisation method in the three-body doubly-heavy-baryon decay.

In summary, a new mode of the doubly-charmed-baryon decay, $\Xi_{cc}^{++} \to \Xi_c^0\pi^+\pi^+$, is observed in a data sample of $pp$ collisions collected by the LHCb experiment at a centre-of-mass energy of 13 TeV, corresponding to an integrated luminosity of 5.4 fb$^{-1}$. The branching fraction ratio between the $\Xi_{cc}^{++} \to \Xi_c^0\pi^+\pi^+$ and $\Xi_{cc}^{++} \to \Lambda_c^+K^-\pi^+\pi^+$ decays is measured for the first time. This measurement provides important information towards an improved understanding of the decays of doubly charmed baryons, and contributes to shed light on the dynamics of low-energy interactions between two confined heavy quarks.

## Acknowledgments

We express our gratitude to our colleagues in the CERN accelerator departments for the excellent performance of the LHC. We thank the technical and administrative staff at the LHCb institutes. We acknowledge support from CERN and from the national agencies: ARC (Australia); CAPES, CNPq, FAPERJ and FINEP (Brazil); MOST and NSFC (China);



JHEP10(2025)136

CNRS/IN2P3 (France); BMBF, DFG and MPG (Germany); INFN (Italy); NWO (Netherlands); MNiSW and NCN (Poland); MCID/IFA (Romania); MICIU and AEI (Spain); SNSF and SER (Switzerland); NASU (Ukraine); STFC (United Kingdom); DOE NP and NSF (USA). We acknowledge the computing resources that are provided by ARDC (Australia), CBPF (Brazil), CERN, IHEP and LZU (China), IN2P3 (France), KIT and DESY (Germany), INFN (Italy), SURF (Netherlands), Polish WLCG (Poland), IFIN-HH (Romania), PIC (Spain), CSCS (Switzerland), and GridPP (United Kingdom). We are indebted to the communities behind the multiple open-source software packages on which we depend. Individual groups or members have received support from Key Research Program of Frontier Sciences of CAS, CAS PIFI, CAS CCEPP, Fundamental Research Funds for the Central Universities, and Sci. & Tech. Program of Guangzhou (China); Minciencias (Colombia); EPLANET, Marie Skłodowska-Curie Actions, ERC and NextGenerationEU (European Union); A*MIDEX, ANR, IPhU and Labex P2IO, and Région Auvergne-Rhône-Alpes (France); Alexander-von-Humboldt Foundation (Germany); ICSC (Italy); Severo Ochoa and María de Maeztu Units of Excellence, GVA, XuntaGal, GENCAT, InTalent-Inditex and Prog. Atracción Talento CM (Spain); SRC (Sweden); the Leverhulme Trust, the Royal Society and UKRI (United Kingdom).

**Data Availability Statement.** This article has no associated data or the data will not be deposited.

**Code Availability Statement.** This article has no associated code or the code will not be deposited.

**Open Access.** This article is distributed under the terms of the Creative Commons Attribution License (CC-BY4.0), which permits any use, distribution and reproduction in any medium, provided the original author(s) and source are credited.

## References

[1] M. Gell-Mann, *A schematic model of baryons and mesons*, *Phys. Lett.* **8** (1964) 214 [INSPIRE].

[2] G. Zweig, *An $SU_3$ model for strong interaction symmetry and its breaking; Version 1*, CERN-TH-401, CERN, Geneva (1964) [DOI:10.17181/CERN-TH-401].

[3] G. Zweig, *An $SU_3$ model for strong interaction symmetry and its breaking; Version 2*, CERN-TH-412 CERN, Geneva (1964) [DOI:10.17181/CERN-TH-412].

[4] A. De Rujula, H. Georgi and S.L. Glashow, *Hadron masses in a gauge theory*, *Phys. Rev. D* **12** (1975) 147 [INSPIRE].

[5] Particle Data Group collaboration, *Review of particle physics*, *Phys. Rev. D* **110** (2024) 030001 [INSPIRE].

[6] LHCb collaboration, *Observation of the doubly charmed baryon $\Xi_{cc}^{++}$*, *Phys. Rev. Lett.* **119** (2017) 112001 [arXiv:1707.01621] [INSPIRE].

[7] LHCb collaboration, *First observation of the doubly charmed baryon decay $\Xi_{cc}^{++} \to \Xi_c^+\pi^+$*, *Phys. Rev. Lett.* **121** (2018) 162002 [arXiv:1807.01919] [INSPIRE].

[8] LHCb collaboration, *Observation of the doubly charmed baryon decay $\Xi_{cc}^{++} \to \Xi_c'^+\pi^+$*, *JHEP* **05** (2022) 038 [arXiv:2202.05648] [INSPIRE].



JHEP10(2025)136

[9] LHCb collaboration, *A search for $\Xi_{cc}^{++} \to D^+pK^-\pi^+$ decays*, JHEP **10** (2019) 124 [arXiv:1905.02421] [INSPIRE].

[10] LHCb collaboration, *Measurement of $\Xi_{cc}^{++}$ production in pp collisions at $\sqrt{s} = 13$ TeV*, Chin. Phys. C **44** (2020) 022001 [arXiv:1910.11316] [INSPIRE].

[11] LHCb collaboration, *Measurement of the lifetime of the doubly charmed baryon $\Xi_{cc}^{++}$*, Phys. Rev. Lett. **121** (2018) 052002 [arXiv:1806.02744] [INSPIRE].

[12] LHCb collaboration, *Precision measurement of the $\Xi_{cc}^{++}$ mass*, JHEP **02** (2020) 049 [arXiv:1911.08594] [INSPIRE].

[13] W. Roberts and M. Pervin, *Heavy baryons in a quark model*, Int. J. Mod. Phys. A **23** (2008) 2817 [arXiv:0711.2492] [INSPIRE].

[14] Z.-G. Wang, *Analysis of the $\frac{1}{2}^+$ doubly heavy baryon states with QCD sum rules*, Eur. Phys. J. A **45** (2010) 267 [arXiv:1001.4693] [INSPIRE].

[15] J.-R. Zhang and M.-Q. Huang, *Doubly heavy baryons in QCD sum rules*, Phys. Rev. D **78** (2008) 094007 [arXiv:0810.5396] [INSPIRE].

[16] C.-H. Chang, C.-F. Qiao, J.-X. Wang and X.-G. Wu, *Estimate of the hadronic production of the doubly charmed baryon $\Xi_{cc}$ under GM-VFN scheme*, Phys. Rev. D **73** (2006) 094022 [hep-ph/0601032] [INSPIRE].

[17] C. Alexandrou and C. Kallidonis, *Low-lying baryon masses using $N_f = 2$ twisted mass clover-improved fermions directly at the physical pion mass*, Phys. Rev. D **96** (2017) 034511 [arXiv:1704.02647] [INSPIRE].

[18] D. Ebert, R.N. Faustov, V.O. Galkin and A.P. Martynenko, *Mass spectra of doubly heavy baryons in the relativistic quark model*, Phys. Rev. D **66** (2002) 014008 [hep-ph/0201217] [INSPIRE].

[19] M. Karliner and J.L. Rosner, *Baryons with two heavy quarks: masses, production, decays, and detection*, Phys. Rev. D **90** (2014) 094007 [arXiv:1408.5877] [INSPIRE].

[20] V.V. Kiselev and A.K. Likhoded, *Baryons with two heavy quarks*, Phys. Usp. **45** (2002) 455 [hep-ph/0103169] [INSPIRE].

[21] T. Gutsche et al., *Analysis of the semileptonic and nonleptonic two-body decays of the double heavy charm baryon states $\Xi_{cc}^{++}$, $\Xi_{cc}^{+}$ and $\Omega_{cc}^{+}$*, Phys. Rev. D **100** (2019) 114037 [arXiv:1911.10785] [INSPIRE].

[22] H.-Y. Cheng, G. Meng, F. Xu and J. Zou, *Two-body weak decays of doubly charmed baryons*, Phys. Rev. D **101** (2020) 034034 [arXiv:2001.04553] [INSPIRE].

[23] F.-S. Yu, *Role of decay in the search for double-charm baryons*, Sci. China Phys. Mech. Astron. **63** (2020) 221065 [arXiv:1912.10253] [INSPIRE].

[24] X.-H. Hu, R.-H. Li and Z.-P. Xing, *A comprehensive analysis of weak transition form factors for doubly heavy baryons in the light front approach*, Eur. Phys. J. C **80** (2020) 320 [arXiv:2001.06375] [INSPIRE].

[25] Y.-J. Shi, W. Wang and Z.-X. Zhao, *QCD sum rules analysis of weak decays of doubly-heavy baryons*, Eur. Phys. J. C **80** (2020) 568 [arXiv:1902.01092] [INSPIRE].

[26] Y.-J. Shi, W. Wang, Y. Xing and J. Xu, *Weak decays of doubly heavy baryons: multi-body decay channels*, Eur. Phys. J. C **78** (2018) 56 [arXiv:1712.03830] [INSPIRE].

[27] Y.-J. Shi, W. Wang, Z.-X. Zhao and U.-G. Meißner, *Towards a heavy diquark effective theory for weak decays of doubly heavy baryons*, Eur. Phys. J. C **80** (2020) 398 [arXiv:2002.02785] [INSPIRE].

JHEP10(2025)136

[28] LHCb collaboration, *The LHCb detector at the LHC*, 2008 *JINST* **3** S08005 [INSPIRE].

[29] LHCb collaboration, *LHCb detector performance*, *Int. J. Mod. Phys. A* **30** (2015) 1530022 [arXiv:1412.6352] [INSPIRE].

[30] R. Aaij et al., *Performance of the LHCb vertex locator*, 2014 *JINST* **9** P09007 [arXiv:1405.7808] [INSPIRE].

[31] P. d'Argent et al., *Improved performance of the LHCb Outer Tracker in LHC Run 2*, 2017 *JINST* **12** P11016 [arXiv:1708.00819] [INSPIRE].

[32] M. Adinolfi et al., *Performance of the LHCb RICH detector at the LHC*, *Eur. Phys. J. C* **73** (2013) 2431 [arXiv:1211.6759] [INSPIRE].

[33] A.A. Alves Jr. et al., *Performance of the LHCb muon system*, 2013 *JINST* **8** P02022 [arXiv:1211.1346] [INSPIRE].

[34] R. Aaij et al., *The LHCb trigger and its performance in 2011*, 2013 *JINST* **8** P04022 [arXiv:1211.3055] [INSPIRE].

[35] R. Aaij et al., *Tesla: an application for real-time data analysis in High Energy Physics*, *Comput. Phys. Commun.* **208** (2016) 35 [arXiv:1604.05596] [INSPIRE].

[36] LHCb collaboration, *Measurement of the $\Lambda_b^0$, $\Xi_b^-$ and $\Omega_b^-$ baryon masses*, *Phys. Rev. Lett.* **110** (2013) 182001 [arXiv:1302.1072] [INSPIRE].

[37] LHCb collaboration, *Precision measurement of D meson mass differences*, *JHEP* **06** (2013) 065 [arXiv:1304.6865] [INSPIRE].

[38] T. Sjostrand, S. Mrenna and P.Z. Skands, *A brief introduction to PYTHIA 8.1*, *Comput. Phys. Commun.* **178** (2008) 852 [arXiv:0710.3820] [INSPIRE].

[39] T. Sjostrand, S. Mrenna and P.Z. Skands, *PYTHIA 6.4 physics and manual*, *JHEP* **05** (2006) 026 [hep-ph/0603175] [INSPIRE].

[40] I. Belyaev et al., *Handling of the generation of primary events in Gauss, the LHCb simulation framework*, *J. Phys. Conf. Ser.* **331** (2011) 032047 [INSPIRE].

[41] C.-H. Chang, J.-X. Wang and X.-G. Wu, *GENXICC2.0: an upgraded version of the generator for hadronic production of double heavy baryons $\Xi_{cc}$, $\Xi_{bc}$ and $\Xi_{bb}$*, *Comput. Phys. Commun.* **181** (2010) 1144 [arXiv:0910.4462] [INSPIRE].

[42] D.J. Lange, *The EvtGen particle decay simulation package*, *Nucl. Instrum. Meth. A* **462** (2001) 152 [INSPIRE].

[43] N. Davidson, T. Przedzinski and Z. Was, *PHOTOS interface in C++: technical and physics documentation*, *Comput. Phys. Commun.* **199** (2016) 86 [arXiv:1011.0937] [INSPIRE].

[44] GEANT4 collaboration, *Geant4 developments and applications*, *IEEE Trans. Nucl. Sci.* **53** (2006) 270 [INSPIRE].

[45] GEANT4 collaboration, *GEANT4 — a simulation toolkit*, *Nucl. Instrum. Meth. A* **506** (2003) 250 [INSPIRE].

[46] M. Clemencic et al., *The LHCb simulation application, Gauss: design, evolution and experience*, *J. Phys. Conf. Ser.* **331** (2011) 032023 [INSPIRE].

[47] L. Breiman, J. Friedman, R.A. Olshen and C.J. Stone, *Classification and regression trees*, Wadsworth international group, Belmont, U.S.A. (1984) [INSPIRE].

[48] Y. Freund and R.E. Schapire, *A decision-theoretic generalization of on-line learning and an application to boosting*, *J. Comput. Syst. Sci.* **55** (1997) 119 [INSPIRE].

JHEP10(2025)136

[49] H. Voss, A. Hocker, J. Stelzer and F. Tegenfeldt, *TMVA, the toolkit for multivariate data analysis with ROOT*, *PoS* **ACAT** (2007) 040 [INSPIRE].

[50] A. Hoecker et al., *TMVA 4 — toolkit for multivariate data analysis with ROOT. Users guide*, physics/0703039 [INSPIRE].

[51] L. Anderlini et al., *The PIDCalib package*, LHCb-PUB-2016-021 (2016).

[52] G. Punzi, *Sensitivity of searches for new signals and its optimization*, *eConf C* **030908** (2003) MODT002 [physics/0308063] [INSPIRE].

[53] T. Skwarnicki, *A study of the radiative cascade transitions between the Upsilon-Prime and Upsilon resonances*, Ph.D. thesis, Institute of Nuclear Physics, Kracow, Poland (1986) [INSPIRE].

[54] G.A. Cowan, D.C. Craik and M.D. Needham, *RapidSim: an application for the fast simulation of heavy-quark hadron decays*, *Comput. Phys. Commun.* **214** (2017) 239 [arXiv:1612.07489] [INSPIRE].

[55] G. Cowan, K. Cranmer, E. Gross and O. Vitells, *Asymptotic formulae for likelihood-based tests of new physics*, *Eur. Phys. J. C* **71** (2011) 1554 [*Erratum ibid.* **73** (2013) 2501] [arXiv:1007.1727] [INSPIRE].

[56] M. Pivk and F.R. Le Diberder, *sPlot: a statistical tool to unfold data distributions*, *Nucl. Instrum. Meth. A* **555** (2005) 356 [physics/0402083] [INSPIRE].

[57] LHCb collaboration, *Measurement of the track reconstruction efficiency at LHCb*, 2015 *JINST* **10** P02007 [arXiv:1408.1251] [INSPIRE].

[58] A. Rogozhnikov, *Reweighting with boosted decision trees*, *J. Phys. Conf. Ser.* **762** (2016) 012036 [arXiv:1608.05806] [INSPIRE].

[59] LHCb collaboration, *Measurement of the mass and lifetime of the $\Omega_b^-$ baryon*, *Phys. Rev. D* **93** (2016) 092007 [arXiv:1604.01412] [INSPIRE].

[60] S.J. Lindenbaum and R.M. Sternheimer, *Isobaric nucleon model for pion production in nucleon-nucleon collisions*, *Phys. Rev.* **105** (1957) 1874 [INSPIRE].

[61] C. Abellán Beteta et al., *Calibration and performance of the LHCb calorimeters in Run 1 and 2 at the LHC*, arXiv:2008.11556 [INSPIRE].

[62] R. Nisius, *On the combination of correlated estimates of a physics observable*, *Eur. Phys. J. C* **74** (2014) 3004 [arXiv:1402.4016] [INSPIRE].

[63] R. Nisius, *BLUE: combining correlated estimates of physics observables within ROOT using the Best Linear Unbiased Estimate method*, arXiv:2001.10310 [DOI:10.1016/j.softx.2020.100468] [INSPIRE].

[64] W. Wang, F.-S. Yu and Z.-X. Zhao, *Weak decays of doubly heavy baryons: the $1/2 \to 1/2$ case*, *Eur. Phys. J. C* **77** (2017) 781 [arXiv:1707.02834] [INSPIRE].

[65] D.-M. Li, X.-R. Zhang, Y. Xing and J. Xu, *Weak decays of doubly heavy baryons: four-body nonleptonic decay channels*, *Eur. Phys. J. Plus* **136** (2021) 772 [arXiv:2101.12574] [INSPIRE].

JHEP10(2025)136

## The LHCb collaboration

R. Aaij[38], A.S.W. Abdelmotteleb[57], C. Abellan Beteta[51], F. Abudinén[57], T. Ackernley[61], A.A. Adefisoye[69], B. Adeva[47], M. Adinolfi[55], P. Adlarson[83], C. Agapopoulou[14], C.A. Aidala[85], Z. Ajaltouni[11], S. Akar[11], K. Akiba[38], P. Albicocco[28], J. Albrecht[19,f], F. Alessio[49], M. Alexander[60], Z. Aliouche[63], P. Alvarez Cartelle[56], R. Amalric[16], S. Amato[3], J.L. Amey[55], Y. Amhis[14], L. An[6], L. Anderlini[27], M. Andersson[51], A. Andreianov[44], P. Andreola[51], M. Andreotti[26], D. Andreou[69], A. Anelli[31,p,49], D. Ao[7], F. Archilli[37,v], M. Argenton[26], S. Arguedas Cuendis[9,49], A. Artamonov[44], M. Artuso[69], E. Aslanides[13], R. Ataíde Da Silva[50], M. Atzeni[65], B. Audurier[12], D. Bacher[64], I. Bachiller Perea[10], S. Bachmann[22], M. Bachmayer[50], J.J. Back[57], P. Baladron Rodriguez[47], V. Balagura[15], A. Balboni[26], W. Baldini[26], L. Balzani[19], H. Bao[7], J. Baptista de Souza Leite[61], C. Barbero Pretel[47,12], M. Barbetti[27], I.R. Barbosa[70], R.J. Barlow[63], M. Barnyakov[25], S. Barsuk[14], W. Barter[59], J. Bartz[69], J.M. Basels[17], S. Bashir[40], B. Batsukh[5], P.B. Battista[14], A. Bay[50], A. Beck[65], M. Becker[19], F. Bedeschi[35], I.B. Bediaga[2], N.A. Behling[19], S. Belin[47], K. Belous[44], I. Belov[29], I. Belyaev[36], G. Benane[13], G. Bencivenni[28], E. Ben-Haim[16], A. Berezhnoy[44], R. Bernet[51], S. Bernet Andres[45], A. Bertolin[33], C. Betancourt[51], F. Betti[59], J. Bex[56], Ia. Bezshyiko[51], O. Bezshyyko[84], J. Bhom[41], M.S. Bieker[19], N.V. Biesuz[26], P. Billoir[16], A. Biolchini[38], M. Birch[62], F.C.R. Bishop[10], A. Bitadze[63], A. Bizzeti[], T. Blake[57], F. Blanc[50], J.E. Blank[19], S. Blusk[69], V. Bocharnikov[44], J.A. Boelhauve[19], O. Boente Garcia[15], T. Boettcher[66], A. Bohare[59], A. Boldyrev[44], C.S. Bolognani[80], R. Bolzonella[26], R.B. Bonacci[1], N. Bondar[44], A. Bordelius[49], F. Borgato[33], S. Borghi[63], M. Borsato[31,p], J.T. Borsuk[41], E. Bottalico[61], S.A. Bouchiba[50], M. Bovill[64], T.J.V. Bowcock[61], A. Boyer[49], C. Bozzi[26], J.D. Brandenburg[86], A. Brea Rodriguez[50], N. Breer[19], J. Brodzicka[41], A. Brossa Gonzalo[47,†], J. Brown[61], D. Brundu[32], E. Buchanan[59], L. Buonincontri[33,q], M. Burgos Marcos[80], A.T. Burke[63], C. Burr[49], J.S. Butter[56], J. Buytaert[49], W. Byczynski[49], S. Cadeddu[32], H. Cai[74], A. Caillet[16], R. Calabrese[26,l], S. Calderon Ramirez[9], L. Calefice[46], S. Cali[28], M. Calvi[31,p], M. Calvo Gomez[45], P. Camargo Magalhaes[2,aa], J. I. Cambon Bouzas[47], P. Campana[28], D.H. Campora Perez[80], A.F. Campoverde Quezada[7], S. Capelli[31], L. Capriotti[26], R. Caravaca-Mora[9], A. Carbone[25,j], L. Carcedo Salgado[47], R. Cardinale[29,n], A. Cardini[32], P. Carniti[31,p], L. Carus[22], A. Casais Vidal[65], R. Caspary[22], G. Casse[61], M. Cattaneo[49], G. Cavallero[26,49], V. Cavallini[26,l], S. Celani[22], S. Cesare[30,o], A.J. Chadwick[61], I. Chahrour[85], H. Chang[4,b], M. Charles[16], Ph. Charpentier[49], E. Chatzianagnostou[38], M. Chefdeville[10], C. Chen[56], S. Chen[5], Z. Chen[7], A. Chernov[41], S. Chernyshenko[53], X. Chiotopoulos[80], V. Chobanova[82], M. Chrzaszcz[41], A. Chubykin[44], V. Chulikov[28,36], P. Ciambrone[28], X. Cid Vidal[47], G. Ciezarek[49], P. Cifra[49], P.E.L. Clarke[59], M. Clemencic[49], H.V. Cliff[56], J. Closier[49], C. Cocha Toapaxi[22], V. Coco[49], J. Cogan[13], E. Cogneras[11], L. Cojocariu[43], S. Collaviti[50], P. Collins[49], T. Colombo[49], M. Colonna[19], A. Comerma-Montells[46], L. Congedo[24], A. Contu[32], N. Cooke[60], C. Coronel[66], I. Corredoira [47], A. Correia[16], G. Corti[49], J. Cottee Meldrum[55], B. Couturier[49], D.C. Craik[51], M. Cruz Torres[2,g], E. Curras Rivera[50], R. Currie[59], C.L. Da Silva[68], S. Dadabaev[44], L. Dai[71], X. Dai[4], E. Dall'Occo[49], J. Dalseno[82], C. D'Ambrosio[49],

JHEP10(2025)136

J. Daniel[11], A. Danilina[44], P. d'Argent[24], G. Darze[3], A. Davidson[57], J.E. Davies[63], O. De Aguiar Francisco[63], C. De Angelis[32,k], F. De Benedetti[49], J. de Boer[38], K. De Bruyn[79], S. De Capua[63], M. De Cian[22], U. De Freitas Carneiro Da Graca[2,a], E. De Lucia[28], J.M. De Miranda[2], L. De Paula[3], M. De Serio[24,h], P. De Simone[28], F. De Vellis[19], J.A. de Vries[80], F. Debernardis[24], D. Decamp[10], V. Dedu[13], S. Dekkers[1], L. Del Buono[16], B. Delaney[65], H.-P. Dembinski[19], J. Deng[8], V. Denysenko[51], O. Deschamps[11], F. Dettori[32,k], B. Dey[77], P. Di Nezza[28], I. Diachkov[44], S. Didenko[44], S. Ding[69], L. Dittmann[22], V. Dobishuk[53], A.D. Docheva[60], C. Dong[4,b], A.M. Donohoe[23], F. Dordei[32], A.C. dos Reis[2], A.D. Dowling[69], W. Duan[72], P. Duda[81], M.W. Dudek[41], L. Dufour[49], V. Duk[34], P. Durante[49], M.M. Duras[81], J.M. Durham[68], O.D. Durmus[77], A. Dziurda[41], A. Dzyuba[44], S. Easo[58], E. Eckstein[18], U. Egede[1], A. Egorychev[44], V. Egorychev[44], S. Eisenhardt[59], E. Ejopu[63], L. Eklund[83], M. Elashri[66], J. Ellbracht[19], S. Ely[62], A. Ene[43], J. Eschle[69], S. Esen[22], T. Evans[63], F. Fabiano[32], L.N. Falcao[2], Y. Fan[7], B. Fang[7], L. Fantini[34,r,49], M. Faria[50], K. Farmer[59], D. Fazzini[31,p], L. Felkowski[81], M. Feng[5,7], M. Feo[2], A. Fernandez Casani[48], M. Fernandez Gomez[47], A.D. Fernez[67], F. Ferrari[25,j], F. Ferreira Rodrigues[3], M. Ferrillo[51], M. Ferro-Luzzi[49], S. Filippov[44], R.A. Fini[24], M. Fiorini[26,l], M. Firlej[40], K.L. Fischer[64], D.S. Fitzgerald[85], C. Fitzpatrick[63], T. Fiutowski[40], F. Fleuret[15], M. Fontana[25], L. F. Foreman[63], R. Forty[49], D. Foulds-Holt[56], V. Franco Lima[3], M. Franco Sevilla[67], M. Frank[49], E. Franzoso[26,l], G. Frau[63], C. Frei[49], D.A. Friday[63], J. Fu[7], Q. Führing[19,f,56], Y. Fujii[1], T. Fulghesu[13], E. Gabriel[38], G. Galati[24], M.D. Galati[38], A. Gallas Torreira[47], D. Galli[25,j], S. Gambetta[59], M. Gandelman[3], P. Gandini[30], B. Ganie[63], H. Gao[7], R. Gao[64], T.Q. Gao[56], Y. Gao[8], Y. Gao[6], Y. Gao[8], L.M. Garcia Martin[50], P. Garcia Moreno[46], J. García Pardiñas[49], P. Gardner[67], K. G. Garg[8], L. Garrido[46], C. Gaspar[49], A. Gavrikov[33], L.L. Gerken[19], E. Gersabeck[63], M. Gersabeck[20], T. Gershon[57], S. Ghizzo[29,n], Z. Ghorbanimoghaddam[55], L. Giambastiani[33,q], F. I. Giasemis[16,e], V. Gibson[56], H.K. Giemza[42], A.L. Gilman[64], M. Giovannetti[28], A. Gioventù[46], L. Girardey[63,58], C. Giugliano[26,l], M.A. Giza[41], F.C. Glaser[14,22], V.V. Gligorov[16,49], C. Göbel[70], L. Golinka-Bezshyyko[84], E. Golobardes[45], D. Golubkov[44], A. Golutvin[62,49,44], S. Gomez Fernandez[46], W. Gomulka[40], F. Goncalves Abrantes[64], M. Goncerz[41], G. Gong[4,b], J.A. Gooding[19], I.V. Gorelov[44], C. Gotti[31], E. Govorkova[65], J.P. Grabowski[18], L.A. Granado Cardoso[49], E. Graugés[46], E. Graverini[50,t], L. Grazette[57], G. Graziani[], A.T. Grecu[43], L.M. Greeven[38], N.A. Grieser[66], L. Grillo[60], S. Gromov[44], C. Gu[15], M. Guarise[26], L. Guerry[11], V. Guliaeva[44], P.A. Günther[22], A.-K. Guseinov[50], E. Gushchin[44], Y. Guz[6,49,44], T. Gys[49], K. Habermann[18], T. Hadavizadeh[1], C. Hadjivasiliou[67], G. Haefeli[50], C. Haen[49], G. Hallett[57], M.M. Halvorsen[49], P.M. Hamilton[67], J. Hammerich[61], Q. Han[33], X. Han[22,49], S. Hansmann-Menzemer[22], L. Hao[7], N. Harnew[64], T. H. Harris[1], M. Hartmann[14], S. Hashmi[40], J. He[7,c], F. Hemmer[49], C. Henderson[66], R.D.L. Henderson[1,57], A.M. Hennequin[49], K. Hennessy[61], L. Henry[50], J. Herd[62], P. Herrero Gascon[22], J. Heuel[17], A. Hicheur[3], G. Hijano Mendizabal[51], J. Horswill[63], R. Hou[8], Y. Hou[11], N. Howarth[61], J. Hu[72], W. Hu[6], X. Hu[4,b], W. Huang[7], W. Hulsbergen[38], R.J. Hunter[57], M. Hushchyn[44], D. Hutchcroft[61], M. Idzik[40], D. Ilin[44], P. Ilten[66], A. Inglessi[44], A. Iniukhin[44],

JHEP10(2025)136

A. Ishteev[44], K. Ivshin[44], R. Jacobsson[49], H. Jage[17], S.J. Jaimes Elles[75,49,48], S. Jakobsen[49], E. Jans[38], B.K. Jashal[48], A. Jawahery[67], V. Jevtic[19,f], E. Jiang[67], X. Jiang[5,7], Y. Jiang[7], Y.J. Jiang[6], M. John[64], A. John Rubesh Rajan[23], D. Johnson[54], C.R. Jones[56], T.P. Jones[57], S. Joshi[42], B. Jost[49], J. Juan Castella[56], N. Jurik[49], I. Juszczak[41], D. Kaminaris[50], S. Kandybei[52], M. Kane[59], Y. Kang[4,b], C. Kar[11], M. Karacson[49], D. Karpenkov[44], A. Kauniskangas[50], J.W. Kautz[66], M.K. Kazanecki[41], F. Keizer[49], M. Kenzie[56], T. Ketel[38], B. Khanji[69], A. Kharisova[44], S. Kholodenko[35,49], G. Khreich[14], T. Kirn[17], V.S. Kirsebom[31,p], O. Kitouni[65], S. Klaver[39], N. Kleijne[35,s], K. Klimaszewski[42], M.R. Kmiec[42], S. Koliiev[53], L. Kolk[19], A. Konoplyannikov[6], P. Kopciewicz[49], P. Koppenburg[38], M. Korolev[44], I. Kostiuk[38], O. Kot[53], S. Kotriakhova, A. Kozachuk[44], P. Kravchenko[44], L. Kravchuk[44], M. Kreps[57], P. Krokovny[44], W. Krupa[69], W. Krzemien[42], O. Kshyvanskyi[53], S. Kubis[81], M. Kucharczyk[41], V. Kudryavtsev[44], E. Kulikova[44], A. Kupsc[83], B. K. Kutsenko[13], D. Lacarrere[49], P. Laguarta Gonzalez[46], A. Lai[32], A. Lampis[32], D. Lancierini[56], C. Landesa Gomez[47], J.J. Lane[1], R. Lane[55], G. Lanfranchi[28], C. Langenbruch[22], J. Langer[19], O. Lantwin[44], T. Latham[57], F. Lazzari[35,t,49], C. Lazzeroni[54], R. Le Gac[13], H. Lee[61], R. Lefèvre[11], A. Leflat[44], S. Legotin[44], M. Lehuraux[57], E. Lemos Cid[49], O. Leroy[13], T. Lesiak[41], E.D. Lesser[49], B. Leverington[22], A. Li[4,b], C. Li[4,b], C. Li[13], H. Li[72], J. Li[8], K. Li[8], L. Li[63], M. Li[8], P. Li[7], P.-R. Li[73], Q. Li[5,7], S. Li[8], T. Li[5,d], T. Li[72], Y. Li[8], Y. Li[5], Z. Lian[4,b], X. Liang[69], S. Libralon[48], C. Lin[7], T. Lin[58], R. Lindner[49], H. Linton[62], V. Lisovskyi[50], R. Litvinov[32,49], D. Liu[8], F.L. Liu[1], G. Liu[72], K. Liu[73], S. Liu[5,7], W. Liu[8], Y. Liu[59], Y. Liu[73], Y.L. Liu[62], G. Loachamin Ordonez[70], A. Lobo Salvia[46], A. Loi[32], T. Long[56], J.H. Lopes[3], A. Lopez Huertas[46], S. López Soliño[47], Q. Lu[15], C. Lucarelli[27,m], D. Lucchesi[33,q], M. Lucio Martinez[80], V. Lukashenko[38,53], Y. Luo[6], A. Lupato[33,i], E. Luppi[26,l], K. Lynch[23], X.-R. Lyu[7], G.M. Ma[4,b], S. Maccolini[19], F. Machefert[14], F. Maciuc[43], B. Mack[69], I. Mackay[64], L.M. Mackey[69], L.R. Madhan Mohan[56], M.J. Madurai[54], A. Maevskiy[44], D. Magdalinski[38], D. Maisuzenko[44], J.J. Malczewski[41], S. Malde[64], L. Malentacca[49], A. Malinin[44], T. Maltsev[44], G. Manca[32,k], G. Mancinelli[13], C. Mancuso[30], R. Manera Escalero[46], F.M. Manganella[37], D. Manuzzi[25], D. Marangotto[30,o], J.F. Marchand[10], R. Marchevski[50], U. Marconi[25], E. Mariani[16], S. Mariani[49], C. Marin Benito[46], J. Marks[22], A.M. Marshall[55], L. Martel[64], G. Martelli[34,r], G. Martellotti[36], L. Martinazzoli[49], M. Martinelli[31,p], D. Martinez Gomez[79], D. Martinez Santos[82], F. Martinez Vidal[48], A. Martorell i Granollers[45], A. Massafferri[2], R. Matev[49], A. Mathad[49], V. Matiunin[44], C. Matteuzzi[69], K.R. Mattioli[15], A. Mauri[62], E. Maurice[15], J. Mauricio[46], P. Mayencourt[50], J. Mazorra de Cos[48], M. Mazurek[42], M. McCann[62], T.H. McGrath[63], N.T. McHugh[60], A. McNab[63], R. McNulty[23], B. Meadows[66], G. Meier[19], D. Melnychuk[42], F.M. Meng[4,b], M. Merk[38,80], A. Merli[50], L. Meyer Garcia[67], D. Miao[5,7], H. Miao[7], M. Mikhasenko[76], D.A. Milanes[75,y], A. Minotti[31,p], E. Minucci[28], T. Miralles[11], B. Mitreska[19], D.S. Mitzel[19], A. Modak[58], L. Moeser[19], R.A. Mohammed[64], R.D. Moise[17], S. Mokhnenko[44], E.F. Molina Cardenas[85], T. Mombächer[49], M. Monk[57,1], S. Monteil[11], A. Morcillo Gomez[47], G. Morello[28], M.J. Morello[35,s], M.P. Morgenthaler[22], J. Moron[40], W. Morren[38], A.B. Morris[49],

JHEP10(2025)136

A.G. Morris[13], R. Mountain[69], H. Mu[4,b], Z.M. Mu[6], E. Muhammad[57], F. Muheim[59], M. Mulder[79], K. Müller[51], F. Muñoz-Rojas[9], R. Murta[62], P. Naik[61], T. Nakada[50], R. Nandakumar[58], T. Nanut[49], I. Nasteva[3], M. Needham[59], E. Nekrasova[44], N. Neri[30,o], S. Neubert[18], N. Neufeld[49], P. Neustroev[44], J. Nicolini[49], D. Nicotra[80], E.M. Niel[49], N. Nikitin[44], Q. Niu[73], P. Nogarolli[3], P. Nogga[18], C. Normand[55], J. Novoa Fernandez[47], G. Nowak[66], C. Nunez[85], H.N. Nur[60], A. Oblakowska-Mucha[40], V. Obraztsov[44], T. Oeser[17], S. Okamura[26,l], A. Okhotnikov[44], O. Okhrimenko[53], R. Oldeman[32,k], F. Oliva[59], M. Olocco[19], C.J.G. Onderwater[80], R.H. O'Neil[49], D. Osthues[19], J.M. Otalora Goicochea[3], P. Owen[51], A. Oyanguren[48], O. Ozcelik[59], F. Paciolla[35,w], A. Padee[42], K.O. Padeken[18], B. Pagare[57], P.R. Pais[22], T. Pajero[49], A. Palano[24], M. Palutan[28], X. Pan[4,b], G. Panshin[5], L. Paolucci[57], A. Papanestis[58,49], M. Pappagallo[24,h], L.L. Pappalardo[26,l], C. Pappenheimer[66], C. Parkes[63], D. Parmar[76], B. Passalacqua[26,l], G. Passaleva[27], D. Passaro[35,s,49], A. Pastore[24], M. Patel[62], J. Patoc[64], C. Patrignani[25,j], A. Paul[69], C.J. Pawley[80], A. Pellegrino[38], J. Peng[5,7], M. Pepe Altarelli[28], S. Perazzini[25], D. Pereima[44], H. Pereira Da Costa[68], A. Pereiro Castro[47], P. Perret[11], A. Perrevoort[79], A. Perro[49,13], M.J. Peters[66], K. Petridis[55], A. Petrolini[29,n], J. P. Pfaller[66], H. Pham[69], L. Pica[35], M. Piccini[34], L. Piccolo[32], B. Pietrzyk[10], G. Pietrzyk[14], R.N. Pilato[61], D. Pinci[36], F. Pisani[49], M. Pizzichemi[31,p,49], V. Placinta[43], M. Plo Casasus[47], T. Poeschl[49], F. Polci[16], M. Poli Lener[28], A. Poluektov[13], N. Polukhina[44], I. Polyakov[63], E. Polycarpo[3], S. Ponce[49], D. Popov[7,49], S. Poslavskii[44], K. Prasanth[59], C. Prouve[82], D. Provenzano[32,k], V. Pugatch[53], G. Punzi[35,t], S. Qasim[51], Q. Q. Qian[6], W. Qian[7], N. Qin[4,b], S. Qu[4,b], R. Quagliani[49], R.I. Rabadan Trejo[57], J.H. Rademacker[55], M. Rama[35], M. Ramírez García[85], V. Ramos De Oliveira[70], M. Ramos Pernas[57], M.S. Rangel[3], F. Ratnikov[44], G. Raven[39], M. Rebollo De Miguel[48], F. Redi[30,i], J. Reich[55], F. Reiss[20], Z. Ren[7], P.K. Resmi[64], M. Ribalda Galvez[46], R. Ribatti[50], G.R. Ricart[15,12], D. Riccardi[35,s], S. Ricciardi[58], K. Richardson[65], M. Richardson-Slipper[59], K. Rinnert[61], P. Robbe[14,49], G. Robertson[60], E. Rodrigues[61], A. Rodriguez Alvarez[46], E. Rodriguez Fernandez[47], J.A. Rodriguez Lopez[75], E. Rodriguez Rodriguez[49], J. Roensch[19], A. Rogachev[44], A. Rogovskiy[58], D.L. Rolf[19], P. Roloff[49], V. Romanovskiy[66], A. Romero Vidal[47], G. Romolini[26], F. Ronchetti[50], T. Rong[6], M. Rotondo[28], S.R. Roy[22], M.S. Rudolph[69], M. Ruiz Diaz[22], R.A. Ruiz Fernandez[47], J. Ruiz Vidal[80], J. Ryzka[40], J.J. Saavedra-Arias[9], J.J. Saborido Silva[47], R. Sadek[15], N. Sagidova[44], D. Sahoo[77], N. Sahoo[54], B. Saitta[32,k], M. Salomoni[31,49,p], I. Sanderswood[48], R. Santacesaria[36], C. Santamarina Rios[47], M. Santimaria[28], L. Santoro [2], E. Santovetti[37], A. Saputi[26,49], D. Saranin[44], A. Sarnatskiy[79], G. Sarpis[59], M. Sarpis[78], C. Satriano[36,u], A. Satta[37], M. Saur[73], D. Savrina[44], H. Sazak[17], F. Sborzacchi[49,28], A. Scarabotto[19], S. Schael[17], S. Scherl[61], M. Schiller[60], H. Schindler[49], M. Schmelling[21], B. Schmidt[49], S. Schmitt[17], H. Schmitz[18], O. Schneider[50], A. Schopper[62], N. Schulte[19], S. Schulte[50], M.H. Schune[14], G. Schwering[17], B. Sciascia[28], A. Sciuccati[49], I. Segal[76], S. Sellam[47], A. Semennikov[44], T. Senger[51], M. Senghi Soares[39], A. Sergi[29,n], N. Serra[51], L. Sestini[27], A. Seuthe[19], Y. Shang[6], D.M. Shangase[85], M. Shapkin[44], R.S. Sharma[69], I. Shchemerov[44], L. Shchutska[50], T. Shears[61], L. Shekhtman[44], Z. Shen[38], S. Sheng[5,7],

JHEP10(2025)136

V. Shevchenko[44], B. Shi[7], Q. Shi[7], Y. Shimizu[14], E. Shmanin[25], R. Shorkin[44], J.D. Shupperd[69], R. Silva Coutinho[69], G. Simi[33,q], S. Simone[24,h], M. Singha[77], N. Skidmore[57], T. Skwarnicki[69], M.W. Slater[54], E. Smith[65], K. Smith[68], M. Smith[62], A. Snoch[38], L. Soares Lavra[59], M.D. Sokoloff[66], F.J.P. Soler[60], A. Solomin[44,55], A. Solovev[44], I. Solovyev[44], N.S. Sommerfeld[18], R. Song[1], Y. Song[50], Y. Song[4,b], Y.S. Song[6], F.L. Souza De Almeida[69], B. Souza De Paula[3], E. Spadaro Norella[29,n], E. Spedicato[25], J.G. Speer[19], E. Spiridenkov[44], P. Spradlin[60], V. Sriskaran[49], F. Stagni[49], M. Stahl[76], S. Stahl[49], S. Stanislaus[64], M. Stefaniak[86], E.N. Stein[49], O. Steinkamp[51], O. Stenyakin[44], H. Stevens[19], D. Strekalina[44], Y. Su[7], F. Suljik[64], J. Sun[32], L. Sun[74], D. Sundfeld[2], W. Sutcliffe[51], K. Swientek[40], F. Swystun[56], A. Szabelski[42], T. Szumlak[40], Y. Tan[4,b], Y. Tang[74], M.D. Tat[22], A. Terentev[44], F. Terzuoli[35,w,49], F. Teubert[49], E. Thomas[49], D.J.D. Thompson[54], H. Tilquin[62], V. Tisserand[11], S. T'Jampens[10], M. Tobin[5,49], L. Tomassetti[26,l], G. Tonani[30,o], X. Tong[6], T. Tork[30], D. Torres Machado[2], L. Toscano[19], D.Y. Tou[4,b], C. Trippl[45], G. Tuci[22], N. Tuning[38], L.H. Uecker[22], A. Ukleja[40], D.J. Unverzagt[22], A. Upadhyay[77], B. Urbach[59], A. Usachov[39], A. Ustyuzhanin[44], U. Uwer[22], V. Vagnoni[25], V. Valcarce Cadenas[47], G. Valenti[25], N. Valls Canudas[49], J. van Eldik[49], H. Van Hecke[68], E. van Herwijnen[62], C.B. Van Hulse[47,z], R. Van Laak[50], M. van Veghel[38], G. Vasquez[51], R. Vazquez Gomez[46], P. Vazquez Regueiro[47], C. Vázquez Sierra[47], S. Vecchi[26], J.J. Velthuis[55], M. Veltri[27,x], A. Venkateswaran[50], M. Verdoglia[32], M. Vesterinen[57], D. Vico Benet[64], P. Vidrier Villalba[46], M. Vieites Diaz[47], X. Vilasis-Cardona[45], E. Vilella Figueras[61], A. Villa[25], P. Vincent[16], B. Vivacqua[3], F.C. Volle[54], D. vom Bruch[13], N. Voropaev[44], K. Vos[80], C. Vrahas[59], J. Wagner[19], J. Walsh[35], E.J. Walton[1,57], G. Wan[6], C. Wang[22], G. Wang[8], H. Wang[73], J. Wang[6], J. Wang[5], J. Wang[4,b], J. Wang[74], M. Wang[49], N.W. Wang[7], R. Wang[55], X. Wang[8], X. Wang[72], X.W. Wang[62], Y. Wang[6], Y.W. Wang[73], Z. Wang[14], Z. Wang[4,b], Z. Wang[30], J.A. Ward[57,1], M. Waterlaat[49], N.K. Watson[54], D. Websdale[62], Y. Wei[6], J. Wendel[82], B.D.C. Westhenry[55], C. White[56], M. Whitehead[60], E. Whiter[54], A.R. Wiederhold[63], D. Wiedner[19], G. Wilkinson[64], M.K. Wilkinson[66], M. Williams[65], M.J. Williams[49], M.R.J. Williams[59], R. Williams[56], Z. Williams[55], F.F. Wilson[58], M. Winn[12], W. Wislicki[42], M. Witek[41], L. Witola[19], G. Wormser[14], S.A. Wotton[56], H. Wu[69], J. Wu[8], X. Wu[74], Y. Wu[6,56], Z. Wu[7], K. Wyllie[49], S. Xian[72], Z. Xiang[5], Y. Xie[8], T.X. Xing[30], A. Xu[35], L. Xu[4,b], L. Xu[4,b], M. Xu[57], Z. Xu[49], Z. Xu[7], Z. Xu[5], K. Yang[62], S. Yang[7], X. Yang[6], Y. Yang[29,n], Z. Yang[6], V. Yeroshenko[14], H. Yeung[63], H. Yin[8], X. Yin[7], C.Y. Yu[6], J. Yu[71], X. Yuan[5], Y Yuan[5,7], E. Zaffaroni[50], M. Zavertyaev[21], M. Zdybal[41], F. Zenesini[25], C. Zeng[5,7], M. Zeng[4,b], C. Zhang[6], D. Zhang[8], J. Zhang[7], L. Zhang[4,b], S. Zhang[71], S. Zhang[64], Y. Zhang[6], Y.Z. Zhang[4,b], Z. Zhang[4,b], Y. Zhao[22], A. Zhelezov[22], S.Z. Zheng[6], X.Z. Zheng[4,b], Y. Zheng[7], T. Zhou[6], X. Zhou[8], Y. Zhou[7], V. Zhovkovska[57], L.Z. Zhu[7], X. Zhu[4,b], X. Zhu[8], V. Zhukov[17], J. Zhuo[48], Q. Zou[5,7], D. Zuliani[33,q], G. Zunica[50]

[1] *School of Physics and Astronomy, Monash University, Melbourne, Australia*
[2] *Centro Brasileiro de Pesquisas Físicas (CBPF), Rio de Janeiro, Brazil*
[3] *Universidade Federal do Rio de Janeiro (UFRJ), Rio de Janeiro, Brazil*
[4] *Department of Engineering Physics, Tsinghua University, Beijing, China*
[5] *Institute Of High Energy Physics (IHEP), Beijing, China*

JHEP10(2025)136

[6] School of Physics State Key Laboratory of Nuclear Physics and Technology, Peking University, Beijing, China
[7] University of Chinese Academy of Sciences, Beijing, China
[8] Institute of Particle Physics, Central China Normal University, Wuhan, Hubei, China
[9] Consejo Nacional de Rectores (CONARE), San Jose, Costa Rica
[10] Université Savoie Mont Blanc, CNRS, IN2P3-LAPP, Annecy, France
[11] Université Clermont Auvergne, CNRS/IN2P3, LPC, Clermont-Ferrand, France
[12] Université Paris-Saclay, Centre d'Etudes de Saclay (CEA), IRFU, Saclay, France, Gif-Sur-Yvette, France
[13] Aix Marseille Univ, CNRS/IN2P3, CPPM, Marseille, France
[14] Université Paris-Saclay, CNRS/IN2P3, IJCLab, Orsay, France
[15] Laboratoire Leprince-Ringuet, CNRS/IN2P3, Ecole Polytechnique, Institut Polytechnique de Paris, Palaiseau, France
[16] LPNHE, Sorbonne Université, Paris Diderot Sorbonne Paris Cité, CNRS/IN2P3, Paris, France
[17] I. Physikalisches Institut, RWTH Aachen University, Aachen, Germany
[18] Universität Bonn - Helmholtz-Institut für Strahlen und Kernphysik, Bonn, Germany
[19] Fakultät Physik, Technische Universität Dortmund, Dortmund, Germany
[20] Physikalisches Institut, Albert-Ludwigs-Universität Freiburg, Freiburg, Germany
[21] Max-Planck-Institut für Kernphysik (MPIK), Heidelberg, Germany
[22] Physikalisches Institut, Ruprecht-Karls-Universität Heidelberg, Heidelberg, Germany
[23] School of Physics, University College Dublin, Dublin, Ireland
[24] INFN Sezione di Bari, Bari, Italy
[25] INFN Sezione di Bologna, Bologna, Italy
[26] INFN Sezione di Ferrara, Ferrara, Italy
[27] INFN Sezione di Firenze, Firenze, Italy
[28] INFN Laboratori Nazionali di Frascati, Frascati, Italy
[29] INFN Sezione di Genova, Genova, Italy
[30] INFN Sezione di Milano, Milano, Italy
[31] INFN Sezione di Milano-Bicocca, Milano, Italy
[32] INFN Sezione di Cagliari, Monserrato, Italy
[33] INFN Sezione di Padova, Padova, Italy
[34] INFN Sezione di Perugia, Perugia, Italy
[35] INFN Sezione di Pisa, Pisa, Italy
[36] INFN Sezione di Roma La Sapienza, Roma, Italy
[37] INFN Sezione di Roma Tor Vergata, Roma, Italy
[38] Nikhef National Institute for Subatomic Physics, Amsterdam, Netherlands
[39] Nikhef National Institute for Subatomic Physics and VU University Amsterdam, Amsterdam, Netherlands
[40] AGH - University of Krakow, Faculty of Physics and Applied Computer Science, Kraków, Poland
[41] Henryk Niewodniczanski Institute of Nuclear Physics Polish Academy of Sciences, Kraków, Poland
[42] National Center for Nuclear Research (NCBJ), Warsaw, Poland
[43] Horia Hulubei National Institute of Physics and Nuclear Engineering, Bucharest-Magurele, Romania
[44] Authors affiliated with an institute formerly covered by a cooperation agreement with CERN.
[45] DS4DS, La Salle, Universitat Ramon Llull, Barcelona, Spain
[46] ICCUB, Universitat de Barcelona, Barcelona, Spain
[47] Instituto Galego de Física de Altas Enerxías (IGFAE), Universidade de Santiago de Compostela, Santiago de Compostela, Spain
[48] Instituto de Fisica Corpuscular, Centro Mixto Universidad de Valencia - CSIC, Valencia, Spain
[49] European Organization for Nuclear Research (CERN), Geneva, Switzerland
[50] Institute of Physics, Ecole Polytechnique Fédérale de Lausanne (EPFL), Lausanne, Switzerland
[51] Physik-Institut, Universität Zürich, Zürich, Switzerland
[52] NSC Kharkiv Institute of Physics and Technology (NSC KIPT), Kharkiv, Ukraine
[53] Institute for Nuclear Research of the National Academy of Sciences (KINR), Kyiv, Ukraine
[54] School of Physics and Astronomy, University of Birmingham, Birmingham, United Kingdom
[55] H.H. Wills Physics Laboratory, University of Bristol, Bristol, United Kingdom

JHEP10(2025)136

[56] Cavendish Laboratory, University of Cambridge, Cambridge, United Kingdom
[57] Department of Physics, University of Warwick, Coventry, United Kingdom
[58] STFC Rutherford Appleton Laboratory, Didcot, United Kingdom
[59] School of Physics and Astronomy, University of Edinburgh, Edinburgh, United Kingdom
[60] School of Physics and Astronomy, University of Glasgow, Glasgow, United Kingdom
[61] Oliver Lodge Laboratory, University of Liverpool, Liverpool, United Kingdom
[62] Imperial College London, London, United Kingdom
[63] Department of Physics and Astronomy, University of Manchester, Manchester, United Kingdom
[64] Department of Physics, University of Oxford, Oxford, United Kingdom
[65] Massachusetts Institute of Technology, Cambridge, MA, United States
[66] University of Cincinnati, Cincinnati, OH, United States
[67] University of Maryland, College Park, MD, United States
[68] Los Alamos National Laboratory (LANL), Los Alamos, NM, United States
[69] Syracuse University, Syracuse, NY, United States
[70] Pontifícia Universidade Católica do Rio de Janeiro (PUC-Rio), Rio de Janeiro, Brazil, associated to [3]
[71] School of Physics and Electronics, Hunan University, Changsha City, China, associated to [8]
[72] Guangdong Provincial Key Laboratory of Nuclear Science, Guangdong-Hong Kong Joint Laboratory of Quantum Matter, Institute of Quantum Matter, South China Normal University, Guangzhou, China, associated to [4]
[73] Lanzhou University, Lanzhou, China, associated to [5]
[74] School of Physics and Technology, Wuhan University, Wuhan, China, associated to [4]
[75] Departamento de Fisica , Universidad Nacional de Colombia, Bogota, Colombia, associated to [16]
[76] Ruhr Universitaet Bochum, Fakultaet f. Physik und Astronomie, Bochum, Germany, associated to [19]
[77] Eotvos Lorand University, Budapest, Hungary, associated to [49]
[78] Vilnius University, Vilnius, Lithuania, associated to [20]
[79] Van Swinderen Institute, University of Groningen, Groningen, Netherlands, associated to [38]
[80] Universiteit Maastricht, Maastricht, Netherlands, associated to [38]
[81] Tadeusz Kosciuszko Cracow University of Technology, Cracow, Poland, associated to [41]
[82] Universidade da Coruña, A Coruña, Spain, associated to [45]
[83] Department of Physics and Astronomy, Uppsala University, Uppsala, Sweden, associated to [60]
[84] Taras Schevchenko University of Kyiv, Faculty of Physics, Kyiv, Ukraine, associated to [14]
[85] University of Michigan, Ann Arbor, MI, United States, associated to [69]
[86] Ohio State University, Columbus, United States, associated to [68]

[a] Centro Federal de Educacão Tecnológica Celso Suckow da Fonseca, Rio De Janeiro, Brazil
[b] Center for High Energy Physics, Tsinghua University, Beijing, China
[c] Hangzhou Institute for Advanced Study, UCAS, Hangzhou, China
[d] School of Physics and Electronics, Henan University , Kaifeng, China
[e] LIP6, Sorbonne Université, Paris, France
[f] Lamarr Institute for Machine Learning and Artificial Intelligence, Dortmund, Germany
[g] Universidad Nacional Autónoma de Honduras, Tegucigalpa, Honduras
[h] Università di Bari, Bari, Italy
[i] Università di Bergamo, Bergamo, Italy
[j] Università di Bologna, Bologna, Italy
[k] Università di Cagliari, Cagliari, Italy
[l] Università di Ferrara, Ferrara, Italy
[m] Università di Firenze, Firenze, Italy
[n] Università di Genova, Genova, Italy
[o] Università degli Studi di Milano, Milano, Italy
[p] Università degli Studi di Milano-Bicocca, Milano, Italy
[q] Università di Padova, Padova, Italy
[r] Università di Perugia, Perugia, Italy
[s] Scuola Normale Superiore, Pisa, Italy
[t] Università di Pisa, Pisa, Italy

JHEP10(2025)136

[u] *Università della Basilicata, Potenza, Italy*
[v] *Università di Roma Tor Vergata, Roma, Italy*
[w] *Università di Siena, Siena, Italy*
[x] *Università di Urbino, Urbino, Italy*
[y] *Universidad de Ingeniería y Tecnología (UTEC), Lima, Peru*
[z] *Universidad de Alcalá, Alcalá de Henares , Spain*
[aa] *Facultad de Ciencias Fisicas, Madrid, Spain*
[†] *Deceased*

JHEP10(2025)136